engineering proceedings

MDPI

Proceeding Paper

An Innovative Winding Number Method for Nonlinear Dynamical System Characterization †

Zhengyuan Zhang [1], Shixuan Lu [2], Liming Dai [1,*] and Na Jia [2,*]

[1] Program of Industrial Systems Engineering, Faculty of Engineering and Applied Sciences, University of Regina, Regina, SK S4S 0A2, Canada
[2] Program of Energy Systems Engineering, Faculty of Engineering and Applied Sciences, University of Regina, Regina, SK S4S 0A2, Canada; lu329@uregina.ca
* Correspondence: liming.dai@uregina.ca (L.D.); na.jia@uregina.ca (N.J.)
† Presented at the 1st International Conference on Industrial, Manufacturing, and Process Engineering (ICIMP-2024), Regina, Canada, 27–29 June 2024.

Abstract: The conventional winding number method is extended in this research to characterize the nonlinear dynamical systems, especially in differentiating partially predictable chaos from strong chaos. On modern robotics' challenges with increased degrees of freedom, traditional methods like the Lyapunov exponent are insufficient for distinguishing between strong and partially predictable chaos. The proposed methods examine the winding number's sensitivity with respect to the center and its standard deviations across time sequences to assess predictability and differentiate between different motion types. The Duffing–Van der Pol system is used to show the effectiveness in identifying different chaotic behaviours, offering significant implications for the control of complex robotic systems.

Keywords: nonlinear dynamical characterization; Poincaré map; partially predictable chaos; winding number

check for updates

Citation: Zhang, Z.; Lu, S.; Dai, L.; Jia, N. An Innovative Winding Number Method for Nonlinear Dynamical System Characterization. *Eng. Proc.* **2024**, *76*, 87. https://doi.org/10.3390/engproc2024076087

Academic Editors: Golam Kabir, Sharfuddin Khan, Mohammad Khondoker and Hussameldin Ibrahim

Published: 20 November 2024

Copyright: © 2024 by the authors. Licensee MDPI, Basel, Switzerland. This article is an open access article distributed under the terms and conditions of the Creative Commons Attribution (CC BY) license (https://creativecommons.org/licenses/by/4.0/).

1. Introduction

In modern robotics, the degree of freedom of the structure is largely increased [1,2]. It has been shown that high degrees of freedom allow robots to perform complex operations with precision [3,4]. A higher degree of freedom also helps robots to achieve their tasks effectively and efficiently [5]. In practice, a high degree of freedom is introduced by more links, using parallelogram mechanisms [6], and soft tissues such as robotic grippers [7]. With the increase in degrees of freedom, the control of the robot becomes more challenging.

The study of human behaviour found that when repeating simple motions, human action will not repeat these precisely but show a limited range of variety [8,9]. This phenomenon is particularly intriguing to robotics researchers, as it reflects a simple fact that when the degree of freedom is high, the supposed repetitive motion of a robotic structure may not be periodic but rather chaotic [10,11]. In fact, it is widely accepted that our understanding of human interaction and manipulation of objects remains an open question and a mystery. How humans can operate objects chaotically but also accurately requires further explanation [12].

Therefore, in modern robotics, chaos is inevitably ubiquitous, and when analyzed accurately, many seemingly periodic motions can actually be chaotic [13]. For this reason, it is more important to describe and diagnose partially predictable chaos from strongly chaotic motion [14]. In contrast, the difference between periodic and partially predictable chaotic motion is less of a concern. Therefore, it is of great importance to diagnose how predictable a motion is.

In traditional nonlinear dynamical system analysis, many methods have been dedicated to diagnosing chaotic behaviour. Some classic methods include the Lyapunov

exponent, Kolmogorov entropy, Poincaré map, close return plot, etc. Many of the methods, such as the Lyapunov exponent, focus too much on the local divergence of the trajectories while failing to capture the fact that the motion is, on a large scale, predictable and regular [15,16]. In other words, they are good at differentiating periodicity from chaos but fail to differentiate partially predictable chaos from strong chaos. Some other methods, such as the close return plot and Kolmogorov entropy, are capable of differentiating predictable chaos from strong chaos but fail to do so with a small group of data [17,18].

Wernecke et al. provided an index that can be used to test and describe the predictability of dynamical systems [19]. Vallejo and Sanjuan systematically discussed the applicability of another index. Though these works are pioneers in the field, they are still based on the Lyapunov exponent and are subjected to the choice of tolerance [20].

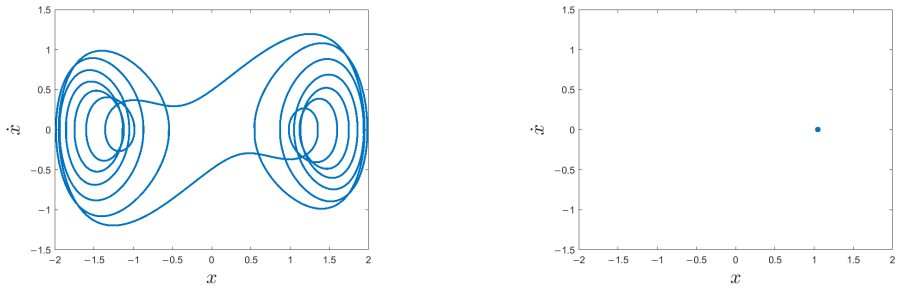
The authors aspire to propose a new method that can automatically analyze the features of the time sequence and provide a quantitative index that describes the predictability of the motion, even within limited periods of motion. For this reason, an innovative winding number method is proposed for dynamical system characterization. This method uses the standard deviation of the winding number in different time sequences to evaluate the predictability of the system and characterize the similarities between periodic and partially predictable motions. It will be shown that the proposed method can be reliable and robust on the assigned task.

2. Methodology

The Duffing–Van der Pol system is an ideal system that can be used as an example of a dynamical system that shows a variety of behaviours. The governing equation of the system is as follows:

$$\ddot{x} - \mu\left(1 - x^2\right)\dot{x} + \alpha x + \beta x^3 = f\cos\omega t \tag{1}$$

To compare with the literature, $\alpha = -0.5$, $\beta = 0.5$, and $\mu = 0.1$ are used [21–23]. Figure 1 shows the difference between the Poincaré maps and phase portraits of the behaviours. When choosing $f = 1$, $\omega = 0.1$, the system is periodic; when $f = 1$, $\omega = 0.5$, the system is quasiperiodic; when $f = 1$, $\omega = 0.2$, the system is partially predictable chaotic; and when $f = 0.2$, $\omega = 0.5$, the system is strongly chaotic. Figure 2 compares the time sequence of the partially predictable chaos and the strong chaos. It can be seen that when $f = 1$, $\omega = 0.2$, the system is predictable chaotic, the period of the system is easy to determine, and the waveform of each period is relatively similar. But when $f = 0.2$, $\omega = 0.5$, the system is strongly chaotic, each period of the system shows a great difference, and the clear range of each period is hard to determine.



(**a**) (**b**)

Figure 1. *Cont.*

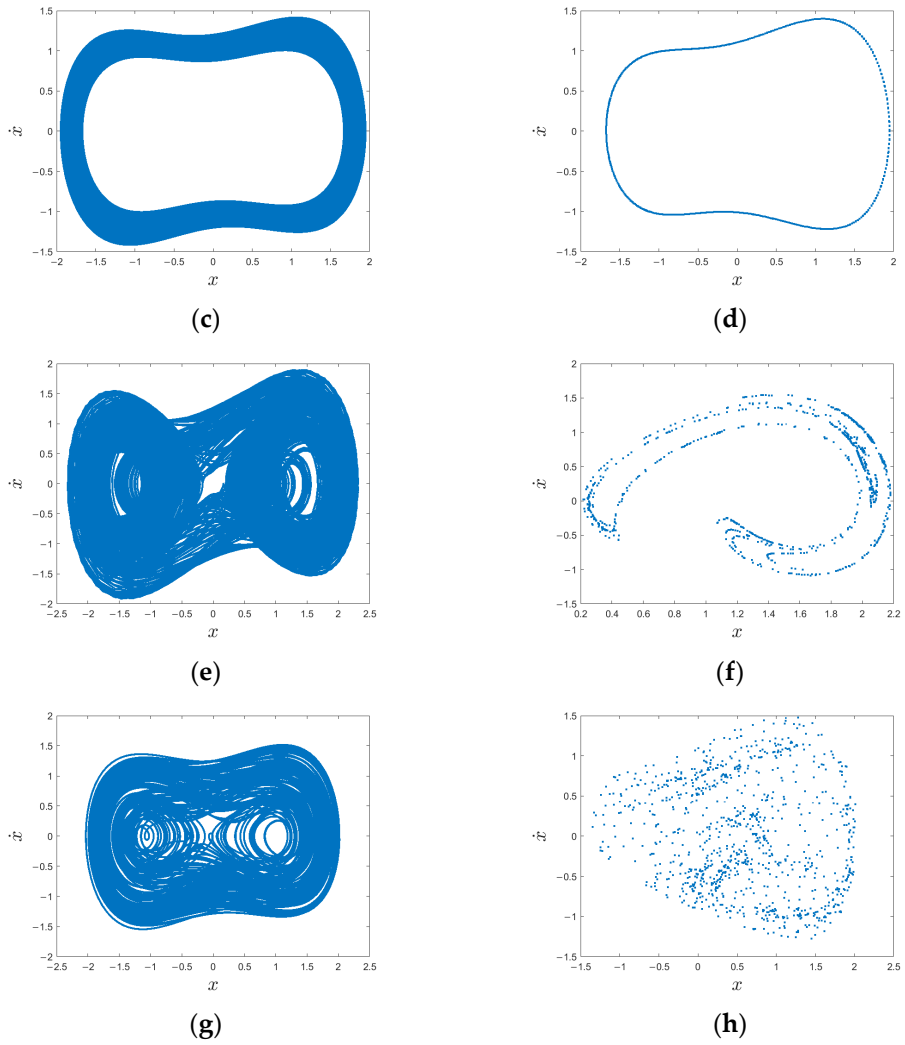


Figure 1. The phase portraits and Poincaré maps of periodic (**a**,**b**), quasiperiodic (**c**,**d**), partially predictable chaotic (**e**,**f**), and strongly chaotic (**g**,**h**) DVP systems [22,23].

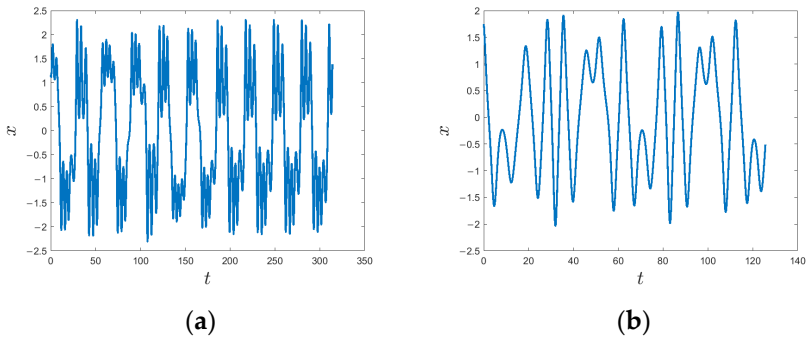


Figure 2. Comparison of partially predictable chaotic (**a**) and strongly chaotic (**b**) DVP systems.

2.1. Sensitivity of the Winding Number

The winding number is a very common way to describe the motion of dynamical systems. However, it is commonly accepted that the winding number is more applicable to the periodic and quasiperiodic systems, while it is hard to rigorously determine the winding number of a chaotic system. However, there are still practical ways to achieve this goal. The most intuitive way is to define:

$$R = \text{wind}(p) = \lim_{n\to\infty} \frac{\theta_n^p - \theta_0^p}{2\pi n} \tag{2}$$

where

$$\theta_n^p = \text{atan2}(y_n^p - y_c, x_n^p - x_c) \tag{3}$$

is the relative angle of the Poincaré point (x_n^p, y_n^p) to the given center (x_c, y_c), p is the initial condition, and n is the times of the Poincaré map.

However, it should be noted that the value of the winding number depends on choosing the center point (x_c, y_c). For a periodic or quasiperiodic system, it is easy to choose a representative reference point that makes the result of Equation (2) reflect the nature of the motion. More specifically, the phase portraits are rings and tori; any point inside the ring or torus can be ideal as the reference point and give the same results. As for the chaotic systems, it can be difficult. The phase portrait can still resemble tori for the partially predictable system. Namely, there are "holes" in the phase portrait, and a reference point in the "holes" can still reflect the nature of the system. However, there is no good option for a strongly chaotic system.

This difference can be further discussed by computing the dependence of the winding number on the choice of reference. Here, the reference is set on the x-axis of the phase space, namely, $y_c = 0$, and the relation between the winding number and the x-coordinate x_c is illustrated, as in Figure 3.

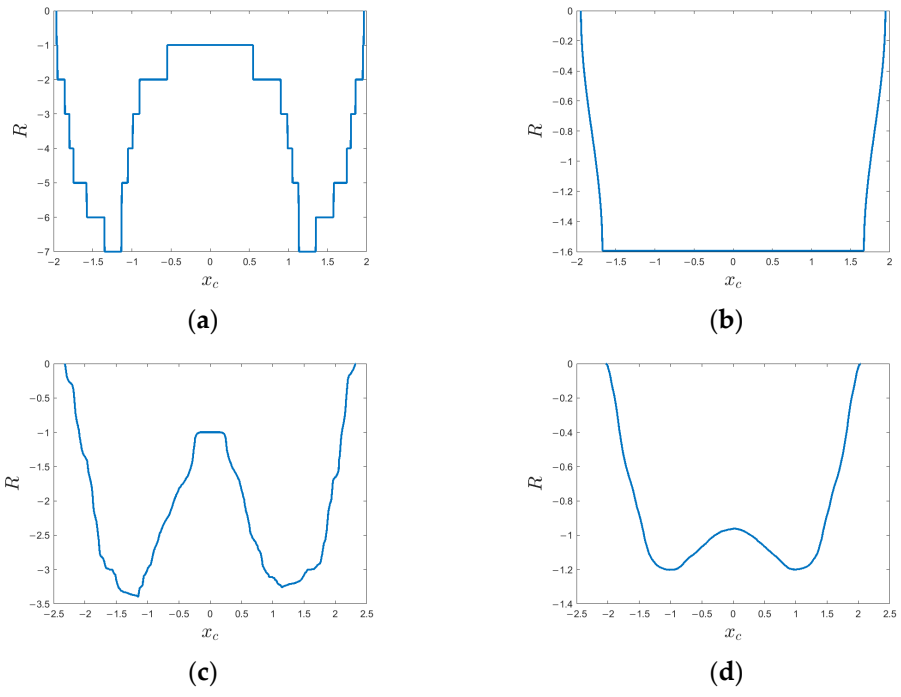


Figure 3. The dependence of the winding number with respect to the location of the center for periodic (**a**), quasiperiodic (**b**), partially predictable chaotic (**c**), and strongly chaotic (**d**) systems.

It is clear that for periodic, quasiperiodic and partially predictable chaotic systems, there is a clear plateau in the relation (which corresponds to the "holes" in their phase portraits), indicating that the change in the reference point location in the range will not cause a change in the value of the winding number. For the strongly chaotic system, differently, as there are no such kind of "holes", the value of the winding number is always sensitive to the location of the center (x_c, y_c).

The curve also reflects whether the excitation is dominant in the system. For the quasiperiodic case in Figure 3b, the value of the plateau is about -1.6, but for the periodic system and partially predictable chaotic system in Figure 3a,c, the winding numbers are

both -1, showing that the excitation is already dominant. For a strongly chaotic system, though there is no clear winding number, it can be seen that when x_c becomes close to 0, the winding number becomes close to -1, also showing the dominant influence of the excitation.

Though the method above is already capable of differentiating different types of chaotic systems, the method faces the limitation that it may require a long-time sequence to check the difference between two systems. The existence of a clear plateau requires an accurate value of the winding number and, therefore, requires the time sequence to be long enough. Nevertheless, the potential of applying the winding number to chaotic systems to differentiate partially predictable chaos from strong chaos has already been shown.

2.2. Standard Deviation of the Winding Number

Another method to differentiate different kinds of chaos is to compute the winding number within a small sequence and see how the winding number computed is sensitive to the initial condition. Instead of computing the limit in Equation (2), the following value is computed.

$$R_{i,n} = \frac{\theta_n^{p_i} - \theta_0^{p_i}}{2\pi n} \tag{4}$$

where $i = 1, 2, \ldots, N$ is the index of a short sequence. Then, the standard deviation of the winding number can be found.

$$R_\sigma(n) = \sqrt{\frac{1}{N}\sum_{i=1}^{N}(R_{i,n} - \mu)^2} \tag{5}$$

Note that this value is a function of sequence length, which is denoted by the number of excitation periods n. By studying the value of R_σ and its relation n, the difference between different systems can be observed. Figure 4 shows the standard deviations and the logarithm of the deviations with respect to n.

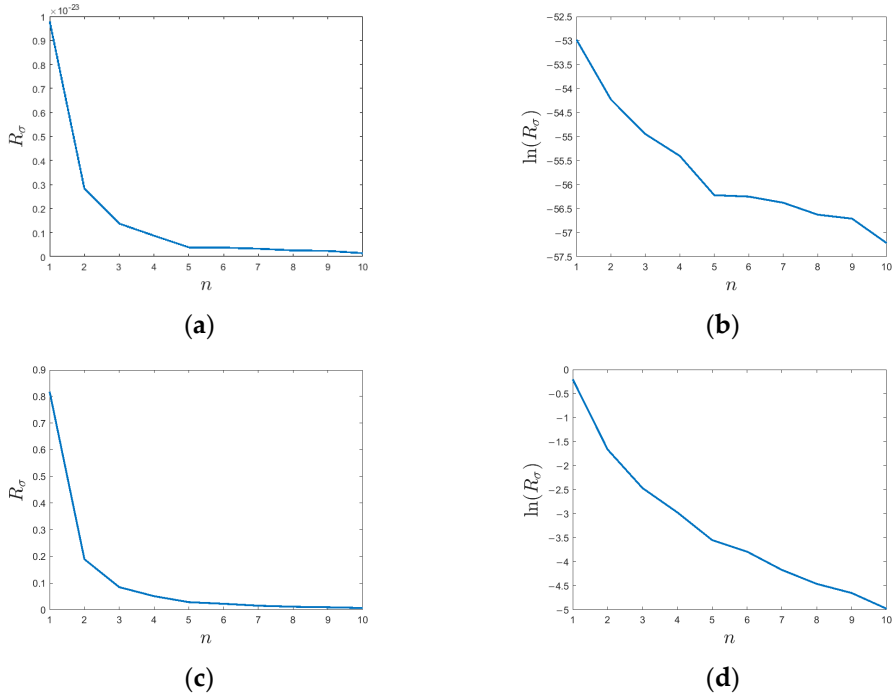


Figure 4. *Cont.*

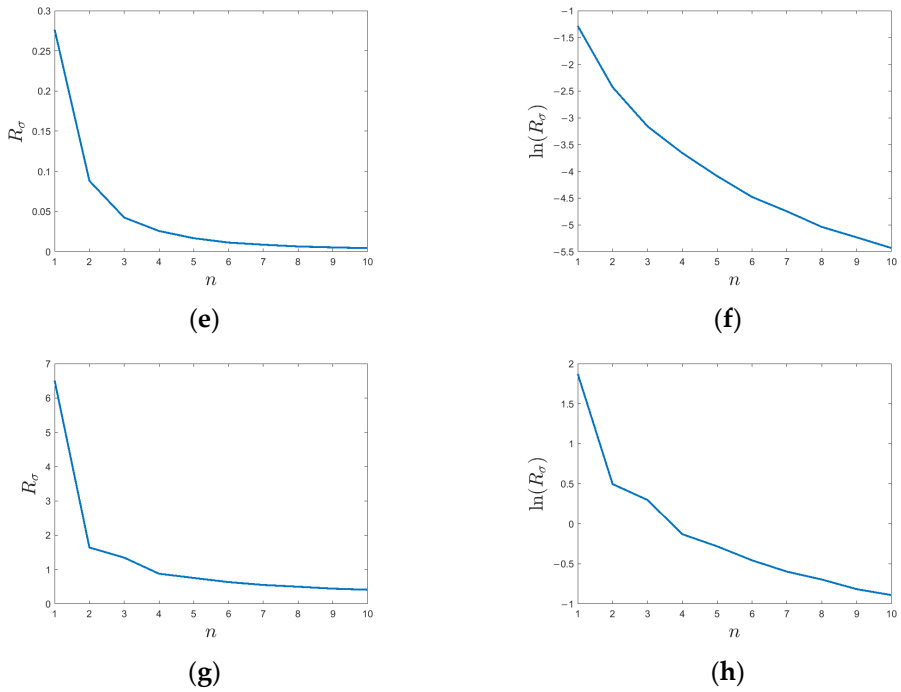


Figure 4. The winding number standard deviations and their logarithms of periodic (**a**,**b**), quasiperiodic (**c**,**d**), partially predictable chaotic (**e**,**f**), and strongly chaotic (**g**,**h**) DVP systems.

In Figure 4, it can be seen that when the system is periodic, all sequences should have exactly the same winding number. Therefore, the deviation is extremely small and only caused by numerical error. As for the quasiperiodic system and partially predictable chaotic system, the value of R_σ can be comparable to 1 when $n = 1$; then, the values decrease exponentially to negligible. For strongly chaotic systems, the initial value can be large, and it does not converge with a clearer exponent but rather converges more slowly as n increases. More details can be found in Table 1. The periodic, quasiperiodic, and partially predictable chaotic systems all have a slope of less than -0.4, while the strongly chaotic system only has one of -0.24. The periodic system is distinguished as the intercept is extremely small. These differences can be directly used as indices that diagnose periodic and strongly chaotic systems, while the quasiperiodic and partially predictable chaotic systems can be diagnosed with other methods. Nevertheless, the main task of determining the predictability of a system is well solved with reliability and accuracy.

Table 1. Slopes and intercepts of the logarithms in Figure 4.

System	Slope	Intercept
periodic	−0.4049	−53.4658
quasiperiodic	−0.4709	−0.6999
partially predictable chaotic	−0.4243	−1.6218
strongly chaotic	−0.2461	1.2327

3. Conclusions

The proposed method provided a systematic process and a practical quantitative index that can be easily used to analyze even a short data sequence. By computing the winding number around different reference points and the standard deviation of the winding number, the strongly chaotic system is separated from other predictable and partially predictable systems.

Author Contributions: Conceptualization, L.D. and Z.Z.; methodology, L.D, Z.Z., N.J. and S.L.; software, Z.Z.; writing—original draft preparation, L.D. and Z.Z.; writing—review and editing, L.D, Z.Z., N.J. and S.L.; visualization, Z.Z.; supervision, L.D. and N.J.; project administration, L.D. and N.J.; funding acquisition, L.D. and N.J. All authors have read and agreed to the published version of the manuscript.

Funding: This research was funded by the Natural Sciences and Engineering Research Council of Canada (NSERC).

Institutional Review Board Statement: Not applicable.

Informed Consent Statement: Not applicable.

Data Availability Statement: Data are contained within the article.

Acknowledgments: The authors greatly appreciate the support of Wuhan Polytechnic University and the University of Regina in the present research.

Conflicts of Interest: The authors declare no conflict of interest.

References

1. Yuan, K.; Chatzinikolaidis, I.; Li, Z. Bayesian optimization for whole-body control of high-degree-of-freedom robots through reduction of dimensionality. *IEEE Robot. Autom. Lett.* **2019**, *4*, 2268–2275. [CrossRef]
2. Kim, D.H.; Lee, Y.; Park, H. Bioinspired high-degrees of freedom soft robotic glove for restoring versatile and comfortable manipulation. *Soft Robot.* **2022**, *9*, 734–744. [CrossRef] [PubMed]
3. Cai, K.; Tian, Y.; Wang, F.; Zhang, D.; Liu, X.; Shirinzadeh, B. Design and control of a 6-degree-of-freedom precision positioning system. *Robot. Comput. Integr. Manuf.* **2017**, *44*, 77–96. [CrossRef]
4. Mauzé, B.; Dahmouche, R.; Laurent, G.J.; André, A.N.; Rougeot, P.; Sandoz, P.; Clévy, C. Nanometer precision with a planar parallel continuum robot. *IEEE Robot. Autom. Lett.* **2020**, *5*, 3806–3813. [CrossRef]
5. Dubey, R.V.; Euler, J.A.; Babcock, S.M. An efficient gradient projection optimization scheme for a seven-degree-of-freedom redundant robot with spherical wrist. In Proceedings of the 1988 IEEE International Conference on Robotics and Automation, Philadelphia, PA, USA, 24–29 April 1988; pp. 28–36.
6. Guo, Y.; Yin, S.; Ren, Y.; Zhu, J.; Yang, S.; Ye, S. A multilevel calibration technique for an industrial robot with parallelogram mechanism. *Precis. Eng.* **2015**, *40*, 261–272. [CrossRef]
7. Tai, K.; El-Sayed, A.; Shahriari, M.; Biglarbegian, M.; Mahmud, S. State of the art robotic grippers and applications. *Robotics* **2016**, *5*, 11. [CrossRef]
8. Stergiou, N.; Decker, L.M. Human movement variability, nonlinear dynamics, and pathology: Is there a connection? *Hum. Mov. Sci.* **2011**, *30*, 869–888. [CrossRef] [PubMed]
9. Lockhart, T.; Stergiou, N. New perspectives in human movement variability. *Ann. Biomed. Eng.* **2013**, *41*, 1593–1594. [CrossRef] [PubMed]
10. Zang, X.; Iqbal, S.; Zhu, Y.; Liu, X.; Zhao, J. Applications of chaotic dynamics in robotics. *Int. J. Adv. Robot. Syst.* **2016**, *13*, 60. [CrossRef]
11. Toz, M. Chaos-based Vortex Search algorithm for solving inverse kinematics problem of serial robot manipulators with offset wrist. *Appl. Soft Comput.* **2020**, *89*, 106074. [CrossRef]
12. Hatze, H. The extended transentropy function as a useful quantifier of human motion variability. *Med. Sci. Sports Exerc.* **1995**, *27*, 751–759. [CrossRef] [PubMed]
13. Lissauer, J.J.; Murray, C.D. Solar system dynamics: Regular and chaotic motion. In *Encyclopedia of the Solar System*; Elsevier: Amsterdam, The Netherlands, 2014; pp. 55–79.
14. Smith, L.A.; Ziehmann, C.; Fraedrich, K. Uncertainty dynamics and predictability in chaotic systems. *Q. J. R. Meteorol. Soc.* **1999**, *125*, 2855–2886. [CrossRef]
15. Aurell, E.; Boffetta, G.; Crisanti, A. Paladin, and A. Vulpiani. Predictability in the large: An extension of the concept of Lyapunov exponent. *J. Phys. A Math. Gen.* **1997**, *30*, 1. [CrossRef]
16. Chen, B.; Li, J.; Ding, R. Nonlinear local Lyapunov exponent and atmospheric predictability research. *Sci. China Ser. D Earth Sci.* **2006**, *49*, 1111–1120. [CrossRef]
17. Yousefpoor, P.; Esfahani, M.S.; Nojumi, H. Looking for systematic approach to select chaos tests. *Appl. Math. Comput.* **2008**, *198*, 73–91. [CrossRef]
18. Anishchenko, V.S.; Astakhov, S. Relative kolmogorov entropy of a chaotic system in the presence of noise. *Int. J. Bifurc. Chaos* **2008**, *18*, 2851–2855. [CrossRef]
19. Wernecke, H.; Sándor, B.; Gros, C. How to test for partially predictable chaos. *Sci. Rep.* **2017**, *7*, 1087. [CrossRef] [PubMed]
20. Vallejo, J.C.; Sanjuán, M.A.F. *Predictability of Chaotic Dynamics*; Springer International Publishing: Berlin/Heidelberg, Germany, 2017.

21. Venkatesan, A.; Lakshmanan, M. Bifurcation and chaos in the double-well Duffing–Van der Pol oscillator: Numerical and analytical studies. *Phys. Rev. E* **1997**, *56*, 6321. [CrossRef]
22. Zhang, Z.; Dai, L. The application of the cell mapping method in the characteristic diagnosis of nonlinear dynamical systems. *Nonlinear Dyn.* **2023**, *111*, 18095–18112. [CrossRef]
23. Zhang, Z.; Dai, L. A box-counting method for characteristic diagnosis of nonlinear dynamical systems. *Int. J. Bifurc. Chaos* **2023**, *33*, 2350139. [CrossRef]

Disclaimer/Publisher's Note: The statements, opinions and data contained in all publications are solely those of the individual author(s) and contributor(s) and not of MDPI and/or the editor(s). MDPI and/or the editor(s) disclaim responsibility for any injury to people or property resulting from any ideas, methods, instructions or products referred to in the content.